

RESEARCH ARTICLE

Open Access



Exosomes promote hFOB1.19 proliferation and differentiation via LINC00520

Jin Wu^{1,2,3}, Licheng Zhang^{1,2*}, Hui Liu³, Jinhui Zhang³ and Peifu Tang^{1,2*}

Abstract

Background Osteoporosis remains a significant clinical challenge worldwide. Recent studies have shown that exosomes stimulate bone regeneration. Thus, it is worthwhile to explore whether exosomes could be a useful therapeutic strategy for osteoporosis. The purpose of this study was to investigate the effects of exosomes derived from human umbilical cord mesenchymal stem cells (hucMSCs) on osteoblast proliferation and differentiation.

Methods Exosomes were isolated from hucMSCs. Bioinformatics analysis was performed to identify the differentially expressed lncRNAs in myeloma-derived mesenchymal stem cells. Plasmids encoding LINC00520 or short hairpin RNA of LINC00520 were transfected into hucMSCs and then exosomes were isolated. After human osteoblasts hFOB1.19 were exposed to the obtained exosomes, cell survival, cell cycle, apoptosis and calcium deposits of hFOB1.19 cell were detected by MTT, 7-aminoactinomycin D, Annexin V-FITC/propidium iodide and Alizarin red staining, respectively.

Results In hFOB1.19 cells, 10×10^9 /mL hucMSC-derived exosomes inhibited cell proliferation, arrested cell cycle, and promoted apoptosis, while hucMSCs or 1×10^9 /mL exosomes promoted cell proliferation, accelerated cell cycle, and promoted calcium deposits and the expression of OCN, RUNX2, collagen I and ALP. In hFOB1.19 cells, exosomes from hucMSCs with LINC00520 knockdown reduced the survival and calcium deposits, arrested the cell cycle, and enhanced the apoptosis, while exosomes from hucMSCs overexpressing LINC00520 enhance the proliferation and calcium deposits and accelerated the cell cycle.

Conclusions LINC00520 functions as a modulator of calcium deposits, and exosomes derived from hucMSCs overexpressing LINC00520 might be a novel therapeutic approach for osteoporosis.

Keywords Osteoblast, Osteoporosis, Human umbilical cord mesenchymal stem cell-derived exosomes, LINC00520

Background

Osteoporosis is a major medical and socioeconomic challenge worldwide, which is characterized by systemic damage to bone mass and microstructure that increases the risk of fragility fractures [1]. Osteoblasts form mineralized bone by producing calcium- and phosphate-based minerals [2]. Thus, direct upregulation of osteoblast proliferation and activity could be an effective way to stimulate bone regeneration and mitigate osteoporosis. Moreover, exosomes have been shown to play important roles in the regulation of osteoblast proliferation and

*Correspondence:

Licheng Zhang
zhanglicheng218@126.com

Peifu Tang

pftang301@163.com

¹ Medical School of Chinese PLA, Chinese PLA General Hospital, No. 28 Fuxing Road, Haidian District, Beijing 100853, China

² Department of Orthopedics, National Clinical Research Center for Orthopedics, Sports Medicine and Rehabilitation, Chinese PLA General Hospital, Beijing 100853, China

³ Department of Orthopedics, The 909th Hospital, School of Medicine, Xiamen University, Zhangzhou 363000, China



© The Author(s) 2023. **Open Access** This article is licensed under a Creative Commons Attribution 4.0 International License, which permits use, sharing, adaptation, distribution and reproduction in any medium or format, as long as you give appropriate credit to the original author(s) and the source, provide a link to the Creative Commons licence, and indicate if changes were made. The images or other third party material in this article are included in the article's Creative Commons licence, unless indicated otherwise in a credit line to the material. If material is not included in the article's Creative Commons licence and your intended use is not permitted by statutory regulation or exceeds the permitted use, you will need to obtain permission directly from the copyright holder. To view a copy of this licence, visit <http://creativecommons.org/licenses/by/4.0/>. The Creative Commons Public Domain Dedication waiver (<http://creativecommons.org/publicdomain/zero/1.0/>) applies to the data made available in this article, unless otherwise stated in a credit line to the data.

activity. Therefore, mesenchymal stem cell (MSC)-derived exosomes may regulate osteoblast differentiation.

Exosomes, 40–160 nm vesicles generated via the endosomal pathway, are secreted by a variety of cells and play a key role in cell–cell communication [3]. Exosomes contain DNA, coding and noncoding RNA, proteins, and antigen presentation molecules that are shuttled between cells [3–7]. Studies have shown that MSC-derived exosomes can induce the differentiation of naïve stem cells into an osteogenic lineage [8]. Exosomes derived from prostate cancer cells can robustly increase human osteoblast proliferation [9], and exosomes derived from human osteosarcoma have been shown to promote the formation of calcium deposits and increase alkaline phosphatase (ALP) activity of osteoblast [10]. Exosomes have been shown to play important roles in the regulation of osteoblast proliferation and activity. Nowadays, emerging studies are focusing on exosomes derived from human umbilical cord mesenchymal stem cell. Human umbilical cord mesenchymal stem cells (hUCMSCs) possess the ability to differentiate into multiple cell types, a property known as pluripotency or multipotency [11]. This differentiation process involves the induction of hUCMSCs with specific growth factors, cytokines, or chemical compounds, which activate signaling pathways and modulate gene expression. Various protocols have been developed to differentiate hUCMSCs into specific lineages such as osteoblasts, adipocytes, chondrocytes, myocytes, and neurons [12–14]. However, whether exosomes from human umbilical cord mesenchymal stem cell (hucMSC-exosomes) exert protective effects against osteoporosis is unknown.

Long non-coding RNAs (lncRNAs) have emerged as novel modulators of MSC osteogenesis [15–17]. Studies showed that MALAT1 delivered by bone marrow-derived MSC-secreted exosomes could alleviate osteoporosis [18], and knockdown of lncRNA BCAR4 was reported to alleviate osteoporosis [19]. The lncRNAs SNHG1, LINC00963, and HOTAIRM1 promoted osteogenic differentiation [20–22]. LINC00520 is a lncRNA that is widely expressed in various tissues and has been linked to the clinicopathological characteristics of 11 cancers [23]; however, its role in osteoblast differentiation has not been explored.

In our study, we co-cultured hucMSC-exosomes with hFOB1.19 human osteoblast cells to explore how these exosomes influence the proliferation and calcium deposits of osteoblasts. Using bioinformatic analysis, we identified LINC00520 as the most highly expressed lncRNA in myeloma-derived MSCs. Silencing and over-expression of LINC00520 showed that LINC00520 plays a crucial role in promoting osteoblast calcium deposits.

Methods

Cell lines

The human osteoblast cell line hFOB1.19 and human umbilical cord mesenchymal stem cells (hucMSCs) were obtained from Xiamen ImmoCell Biotechnology Co., Ltd., and were maintained in dulbecco's modified eagle medium (DMEM)/F12 (catalog number: 12500062, Gibco, Grand Island, USA) supplemented with 10% fetal bovine serum (FBS, catalog number: 10099141C, Gibco) and 1% penicillin–streptomycin (catalog number: 15140148, Gibco). All cells were incubated at 37 °C and 5% CO₂.

Plasmids

The plasmids encoding short hairpin ribonucleic acid (shRNA) of LINC00520 (shLINC00520), the negative control of shLINC00520 (shNC), LINC00520 (LINC00520 OE), or the negative control of LINC00520 OE (Vector) were obtained from Xiamen Antihela Biotechnology Co., Ltd (Xiamen, China). For the construction of plasmids, the shRNA targeting LINC00520 has been inserted into the pLKO.1-TRC vector at the AgeI and EcoRI restriction sites. Furthermore, LINC00520 has been inserted into the plv-cmv-mcs-pGK-puro vector using the EcoRI and BamHI restriction sites. The primers used for plasmid construction are listed in Table 1.

Identification of hucMSCs

To evaluate the surface markers of hucMSCs, hucMSCs at passage three were incubated with antibodies anti-CD34 (catalog number: 343503, BioLegend, San Diego, CA, USA), anti-CD73 (catalog number: 344015, BioLegend), anti-CD29 (catalog number: 303004, BioLegend), anti-CD14 (catalog number: 397706, BioLegend), anti-CD105 (catalog number: 323203, BioLegend), anti-CD19 (catalog number: 302205, BioLegend), anti-CD45 (catalog number: 304005, BioLegend), anti-HLA-DR (catalog number: 327005, BioLegend), and anti-CD90 (catalog number: 328108, BioLegend). Fluorescence was detected using a flow cytometer (NovoCyte 1300; ACEA, San Diego, CA, USA) to identify hucMSCs.

To evaluate cell differentiation, hucMSCs at passage three were cultured in adipogenic (catalog number: A1007001, Gibco, Grand Island, USA), chondrogenic (catalog number: A1007101, Gibco), or osteogenic medium (catalog number: A1007201, Gibco) for 3 weeks. Subsequently, the cells were fixed with 4% paraformaldehyde, and stained with oil red O (catalog number: HY-D1168, MedChemExpress, New Jersey, USA), alcian blue (catalog number: HY-D0001, MedChemExpress), or alizarin red (catalog number:

Table 1 Primers for plasmid construction and RT-qPCR

Primers		Sequence (5'-3')
shLINC00520	F	CCGGGGACTGCAATTCACAAG AACACTCGAGTGTCTTGTA ATTGCAGTCCTTTT
	R	AATTA AAAAGGACTGCAATTC ACAAGA AACTCGAGTGTCT TGTAATTGCAGTCC
LINC00520 OE	F	ATTCGATTCTTGGCTTTA
	R	TTCTTTCCCTGCACTGTAC
HEIH	F	GCAGTAACAGAGTCAACA
	R	CAAGAATTATCGTGGAAACAG
LINC00520	F	GTAAGATATGACTGTGCTC
	R	CATACTCATGGAGTTCCA
LINC00623	F	CAGTTGTTCCAGCATAGTG
	R	ATGTATCCCAGAAACCTAAA
OIP5-AS1	F	AATCAGCAGAGGACCATT
	R	CAGCATCACAGCATTAT
PRR34-AS1	F	GCAGGAATATGACAACAG
	R	GTTATTAAGATGGTAGCAGTT
18S	F	CGACGACCCATTCGAACGTCT
	R	CTCTCCGGAATCGAA CCCTGA
OCN	F	CGCTACCTGTATCAATGGCTGG
	R	CTCTGAAAGCCGATGTGGTCA
RUNX2	F	CCCAGTATGAGAGTAGGTGTC
	R	GGGTAAGACTGGTCATAGGACC
Collagen I	F	GATTCCTGGACCTAAAGGTGC
	R	AGCCTCTCCATCTTGGCCAGCA
ALP	F	AGCGTGACTTGAAGTGTGCAT
	R	GAAAGGACCTGGACCACACAGA

F, forward primer; R, reverse primer

HY-120601, MedChemExpres), respectively. The stained cells were observed under a light microscope (Olympus, Tokyo, Japan).

Extraction, purification, and characterization of hucMSC-exosomes

Exosomes were extracted from the hucMSCs as follows. The hucMSCs were cultured in medium containing 10% FBS which was centrifuged at $100,000\times g$ for 18 h to remove exosomes. After 24 h, the medium was changed to DMEM/F12 without FBS. After one hour, 5 μg plasmid (shLINC00520, shNC, LINC00520 OE, or Vector) was transfected into hucMSCs using ExFect[®] Transfection Reagent (catalog number: T101, Vazyme, Nanjing, China). Six hours after transfection, the medium was replaced with DMEM/F12 containing 10% FBS. The medium was collected 48 h post-transfection to get the supernatant after centrifugation at $600\times g$ for 5 min. By centrifuging at $100,000\times g$ for 60 min using an

ultra-high-speed centrifuge, the pellets were washed and resuspended with phosphate buffered solution (PBS) to obtain the hucMSC-exosomes and stored at $-80^{\circ}C$ until use.

Observation of hucMSC-exosomes under the electron microscope

The prepared hucMSC-exosomes were fixed with 4% glutaraldehyde at $4^{\circ}C$ for 2 h, rinsed three times with 0.1 mol/L PBS and fixed in 1% osmium tetroxide for 2 h. After gradient dehydration of conventional ethanol and acetone, the samples were immersed, embedded, and polymerized in epoxy resin, followed by preparation of 0.5 nm ultrathin sections. After optical location, 60 nm ultrathin sections were prepared, which were then stained with uranium acetate and lead citrate and observed under a JEM-1230 electron microscope (Nihon Denshi, Tokyo, Japan).

Detection of exosome size

A total of 20 μg exosomes were dissolved in 1 mL PBS and swirled for 1 min, so that the exosomes were evenly distributed. Subsequently, the diameter and concentration of exosomes were measured by NanoSight particle tracking analyzer (NTA, Malvern Panalytical, Malvern, UK).

Labeling hucMSC-exosomes with carboxyfluorescein diacetate succinimidyl-ester (CFSE)

CFSE (catalog number: C1031, Beyotime, Shanghai, China) was dissolved in Dimethyl sulfoxide to a concentration of 1 mM. CFSE was added to hucMSC-exosomes at a final concentration of 1 μM and incubated for 4 h at $37^{\circ}C$. The medium was removed after centrifugation at $100,000 g$ for 90 min. Then, 10 mL of PBS was added to the exosome pellet and gently resuspended to ensure proper mixing. Following that, another centrifugation at $100,000 g$ for 90 min was performed to pellet the exosomes once again. Then, CFSE-labeled hucMSC-exosomes were added to hFOB1.19 cells and incubated for 48 h. The cells were stained with a 4',6-diamidino-2-phenylindole solution (DAPI; catalog number: C1005, Beyotime). The signals were observed using a fluorescence microscope (Olympus, Tokyo, Japan).

Co-culture of osteoblasts and hucMSCs or hucMSC-exosomes

Human osteoblasts (hFOB1.19) were seeded into the bottom chamber of 6-well Transwell plates containing DMEM/F12 supplemented with 10% exosome-free FBS at 2×10^4 cells per well. hucMSCs (2×10^4 cells per well), different concentrations of hucMSC-exosomes (1×10^9 /

mL, 5×10^9 /mL or 10×10^9 /mL), or hucMSCs (2×10^4 cells per well) and 10 μ M GW4869, an inhibitor of exosome synthesis/release [24, 25], were added into the upper chamber. After 48 h, hFOB1.19 cells were collected for follow-up experiments.

Immunoblotting

hFOB1.19 cells were collected and lysed in radioimmunoprecipitation assay (catalog number: P0013B, Beyotime) buffer containing protease and phosphatase inhibitor by incubation on ice for 30 min, homogenization, and sonication. The proteins were extracted, and the concentration was determined using a BCA protein assay kit (catalog number: P0011, Beyotime). Samples were then heated at 95 °C for 10 min. Equal protein (20 μ g) was loaded into each well of a 12% SDS-PAGE gel and electrophoresed at 80 V for 1.5 h. The separated proteins were then transferred to PVDF membranes (catalog number: IPVH00010, Millipore, Massachusetts, USA) at 300 mA for 2.5 h. The membrane was blocked with 5% non-fat milk for 1 h and then incubated with CD81 antibody (1:4000, catalog number: 66866-1-Ig, Proteintech), CD9 antibody (1:3000, catalog number: 20597-1-AP, Proteintech), CD63 antibody (1:3000, catalog number: 25682-1-AP, Proteintech), Actin antibody (catalog number: 20536-1-AP, Proteintech, Wuhan, China), OCN antibody (catalog number: Ab133612, Abcam, Cambridge, UK), RUNX2 antibody (catalog number: 20700-1-AP, Proteintech), CoII antibody (catalog number: 27836-1-AP, Proteintech), or ALP antibody (catalog number: 13365-1-AP, Proteintech) overnight at 4 °C. The membrane was then incubated with horseradish peroxidase-linked goat anti-rabbit IgG (catalog number: SA00001-2, Proteintech) for 1 h at room temperature. After washing three times (10 min each), the ECL kit (catalog number: WP20005, Invitrogen, CA, USA) was used to detect the protein bands, which were visualized using X-ray film. The original images of all immunoblotting in this study are in Additional file 1.

MTT assay

After hFOB1.19 cells were co-cultured with hucMSCs or hucMSC-exosomes for 48 h, MTT was added to each well to a final concentration of 0.5% MTT (catalog number: 40201ES72; Yeasen Biotechnology Co. Ltd., Shanghai, China). After incubation for 3 h, the medium in each well was discarded, and 100 μ L of DMSO was added. The plate was incubated on a shaker at 70–100 rpm for 15 min, and then the optical density (OD) was measured at 490 nm using a SpectraMax[®] Absorbance Plate Reader (supplier number: PLUS 384, Molecular Devices, San Francisco, USA).

Cell cycle detection

The hFOB1.19 cells co-cultured with hucMSCs or hucMSC-exosomes for 48 h were detached carefully by trypsin and collected at $500 \times g$ for 5 min. After fixed in ice-cold 70% ethanol (catalog number: 10009218, SinoPharm Group, Beijing, China) at –20 °C for 12 h, the hFOB1.19 cells were incubated with 0.2% Triton X-100 (catalog number: HFH10, Invitrogen) containing 100 μ g/mL RNase A (catalog number: EN0531, Thermo Scientific, MA, USA) at 37 °C for 30 min. 20 mg/mL 7-aminonincomycin D (7-AAD, catalog number: ST515-1 mg, Beyotime) was added to each sample and incubated at 37 °C for 8 min in an incubator. Then, cells were analyzed by flow cytometry (ACEA, San Diego, CA, USA).

Quantitative PCR (qPCR)

Total RNA was extracted from hFOB1.19 cells using TRIzol reagent (catalog number: 15596026, Invitrogen), and the extracted RNA was used for cDNA synthesis using a reverse transcription kit (catalog number: RR036A, Takara, Tokyo, Japan). qPCR was performed using ChamQ SYBR qPCR Master Mix (catalog number: Q311-02, Vazyme) and an AriaMx Real-Time qPCR system (part number: G8830A, Agilent, California, USA). The real-time PCR cycling condition were as follows: stage I: 95 °C for 30 s; stage II: 40 cycles of 95 °C for 10 s and 60 °C for 30 s; stage III: 95 °C for 15 s, 60 °C for 1 min, and 95 °C for 15 s. The primer sequences are shown in Table 1.

Apoptosis detection

The hFOB1.19 cells co-cultured with hucMSCs or hucMSC-exosomes for 48 h were collected by centrifugation at $500 \times g$ for 5 min, and stained for 20 min using an apoptosis detection kit (catalog number: A211-01, Vazyme, Nanjing, Jiangsu, China) according to the merchant instructions. Then, NovoCyte flow cytometry (ACEA, San Diego, CA, USA) and associated software (NovoExpress 1.4.1, ACEA) were used to analyze the apoptosis ratio.

Alizarin red staining

hFOB1.19 cells were seeded into the bottom chamber of 6-well Transwell plates at 2×10^4 cells per well. hucMSCs (2×10^4 cells per well) or 1×10^9 /mL exosomes from hucMSCs transfected with plasmids (shNC, shLINC00520, Vector, or LINC00520 OE) were added into the upper chamber. After 14 days, hFOB1.19 cells were stained with 2% alizarin red (pH 4.2, Sigma-Aldrich, St Louis, MO, USA) for 10 min, and then washed with distilled water. The mineralized nodules were examined with a light microscope (Olympus, Tokyo, Japan).

Bioinformatics analysis

LncRNA data from multiple myeloma-derived MSC was obtained from the gene expression omnibus (GSE118985, <https://www.ncbi.nlm.nih.gov/geo/query/acc.cgi?acc=GSE118985>) and ggplot2 (v3.3.6) was used to plot the graph. The expression levels of the top 10 lncRNAs in multiple myeloma-derived MSCs were at the intersection of lncRNAs from exosome exoRBase (<http://www.exorbase.org/>). Venn diagram was drawn using Venny 2.1 (<https://bioinfo.gp.cnb.csic.es/tools/venny/index.html>).

Statistical analysis

Statistical analyses were conducted using GraphPad Prism software (version 8.0, GraphPad Software Inc.,

CA, USA). Student’s *t*-test (unpaired) was used to compare the differences between two groups for parametric data. One-way analysis of variance followed by Tukey’s test were used for among multiple groups. Statistics were deemed significant at $P < 0.05$.

Results

Verification of hucMSCs and preparation of hucMSC-exosomes

We first cultured hucMSCs and observed their elongated adherent shape using phase-contrast microscopy (Fig. 1A). Next, we performed flow cytometry to confirm the immunophenotype of the hucMSCs. The surface markers CD29, CD73, CD90, and CD105

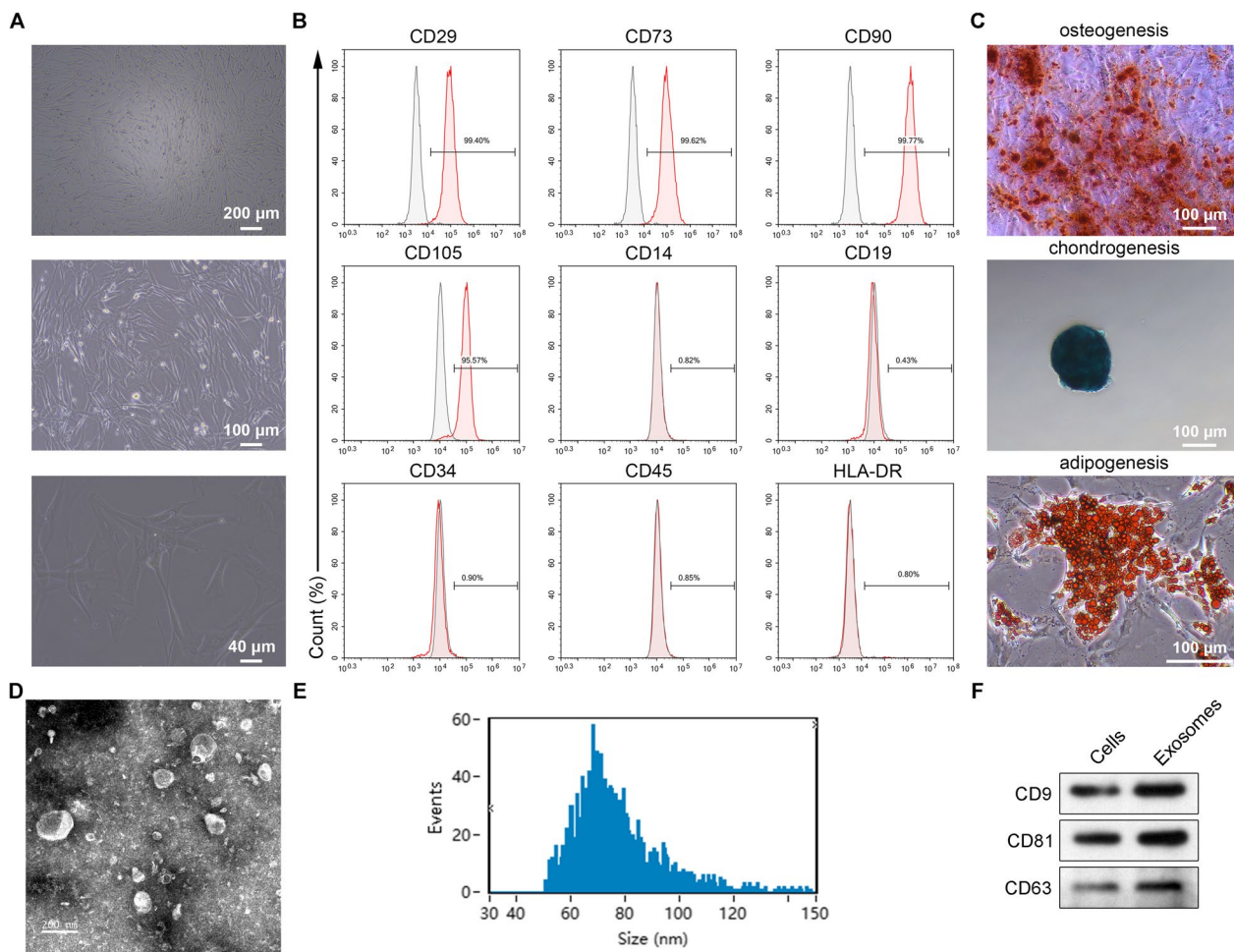


Fig. 1 Identification of human umbilical cord mesenchymal stem cells (hucMSCs) and hucMSC-derived exosomes. **A** The morphology of human umbilical cord-derived MSCs as observed using phase-contrast microscopy. **B** Immunophenotype of human umbilical cord-derived MSCs showing expression of CD29, CD73, CD90, CD105, CD14, CD19, CD34, CD45, and HLA-DR by flow cytometry. **C** Effects of human umbilical cord-derived MSCs on osteogenesis, adipogenesis, and soft tissue formation. **D** Morphology of hucMSC-derived exosomes as determined by transmission electron microscopy. **E** Diameter distribution of hucMSC-exosomes as determined by dynamic light scattering. **F** Immunoblotting of CD9, CD81, CD63, and actin in hucMSCs and derived exosomes

were highly expressed in hucMSCs (Fig. 1B). However, positive expression levels of CD19, CD34, CD45, and HLA-DR were not observed. The multidirectional differentiation potential of hucMSCs was confirmed by osteogenesis, adipogenesis, and chondrogenesis assays. After induction of osteoporosis, adipogenesis, and chondrogenesis, positive staining for alkaline phosphatase, Oil-Red-O, and Von Kossa was observed (Fig. 1C).

We then isolated exosomes from the supernatant of hucMSCs using a previously described method [26]. To verify their identity as exosomes, we first observed their round shape using electron microscopy (Fig. 1D). Then, we used dynamic light scattering, which showed that the size of the hucMSC-exosomes ranged from 50 to 150 nm (Fig. 1E). Finally, immunoblotting showed that CD9, CD63, and CD81 protein levels were higher in hucMSC-exosomes compared to the levels in cells (Fig. 1F). These results confirm that we cultured hucMSCs and isolated exosomes from the hucMSCs successfully.

A low concentration of hucMSC-exosomes promotes the proliferation of osteoblasts

To explore the effect of hucMSC-exosomes on osteoblasts, we treated hFOB1.19 cells with CFSE-labeled hucMSC-exosomes and found that the exosomes could enter hFOB1.19 cells after 48 h of co-culture with CFSE-labeled hucMSC-exosomes (Fig. 2A). To determine whether hucMSCs and hucMSC-exosomes regulate the proliferation of osteoblasts, hFOB1.19 cells were co-cultured with hucMSCs or different concentrations of hucMSC-exosomes for 48 h. The results of an MTT assay indicated that cell viability was increased when cells were co-cultured with hucMSCs or the two lower concentrations of hucMSC-exosomes (1×10^9 /mL and 5×10^9 /mL) compared with control cells, but the highest concentration of exosomes (10×10^9 /mL) had the opposite effect and reduced viability (Fig. 2B). Consistently, when hFOB1.19 cells were co-cultured with hucMSCs or hucMSC-exosomes at lower concentrations (1×10^9 /mL), the number of hFOB1.19 cells in G1 phase decreased (Fig. 2C, D). After co-cultured with hucMSC-exosomes at the highest concentration (10×10^9 /mL), the cell cycle of hFOB1.19 cells was stagnated in G1 phase (Fig. 2C, D). Apoptosis of hFOB1.19 cells was also investigated. The apoptosis was not induced in hFOB1.19 cells cultured with hucMSCs or low-concentration hucMSC-exosomes, while higher apoptosis was induced in hFOB1.19 cells cultured with 10×10^9 /mL hucMSC-exosomes (Fig. 2E, F). These results suggested that high concentration of hucMSC-exosomes inhibited proliferation and induced apoptosis of hFOB1.19 cells.

hucMSCs and hucMSC-exosomes promote calcium deposition in hFOB1.19 cells

Calcium content in hFOB1.19 cells after culture with hucMSCs or hucMSC-exosomes was assessed by Alizarin red staining. hFOB1.19 cells cocultured with 1×10^9 /mL hucMSC-exosomes showed more calcified nodules than cocultured with MSCs (Fig. 3A). The relative mRNA expression levels of marker of late differentiation of osteoblasts OCN, necessary specific transcription factor for osteogenic differentiation RUNX2, and markers of early differentiation of osteoblasts collagen I and ALP were increased in hFOB1.19 cells after co-culture with hucMSCs or hucMSC-exosomes (Fig. 3B). Consistent with the mRNA expression, the protein levels of OCN, RUNX2, collagen I and ALP were significantly upregulated in hFOB1.19 cells after co-culture with hucMSCs or hucMSC-exosomes (Fig. 3C, D). Compared with hucMSCs, hucMSCs-exosomes enhanced the expression of OCN, RUNX2, collagen I and ALP in hFOB1.19 cells (Fig. 3B–D). These findings indicate that hucMSCs and hucMSC-exosomes promote calcium deposition in hFOB1.19 cells.

Identification and validation of the differential expressed lncRNAs in hucMSC-exosomes

To identify the role of lncRNAs in osteoblasts, we performed a bioinformatic analysis. The normalized expression levels of the lncRNAs in the GSE118985 dataset [27] were analyzed (Fig. 4A). The top 10 highly expressed lncRNAs, HEIH, LINC00520, LINC00623, OIP5-AS1, PRR34-AS1, MALAT1, ZFAS1, SNHG19, DANCR, and ITGB2-AS1, were validated in the exorBase database (<http://www.exorbase.org/>) (Fig. 4B). The levels of lncRNA HEIH, LINC00520, LINC00623, OIP5-AS1, and PRR34-AS1 were higher in hucMSC-exosomes than in hucMSCs (Fig. 4C). Further analysis showed that LINC00520, OIP5-AS1, and PRR34-AS1, but not HEIH and LINC00623, were upregulated in hFOB1.19 cells cultured with hucMSCs compared with in hFOB1.19 cells cultured without hucMSCs (Fig. 4D). GW4869 acts as an inhibitor of neutral sphingomyelinase 2 (nSMase2), an enzyme involved in ceramide synthesis [28]. Ceramide is a key lipid component of cellular membranes and plays a regulatory role in various cellular processes, including exosome biogenesis. Inhibition of nSMase2 by GW4869 leads to a reduction in ceramide levels within cells, which subsequently affects the formation and release of exosomes. GW4869 inhibited the up-regulation effect of hucMSCs on HEIH, LINC00520, OIP5-AS1, and PRR34-AS1, but not LINC00623, in hFOB1.19 cells (Fig. 4D). hucMSC-exosomes significantly increased the levels of HEIH, LINC00520, LINC00623, OIP5-AS1, and

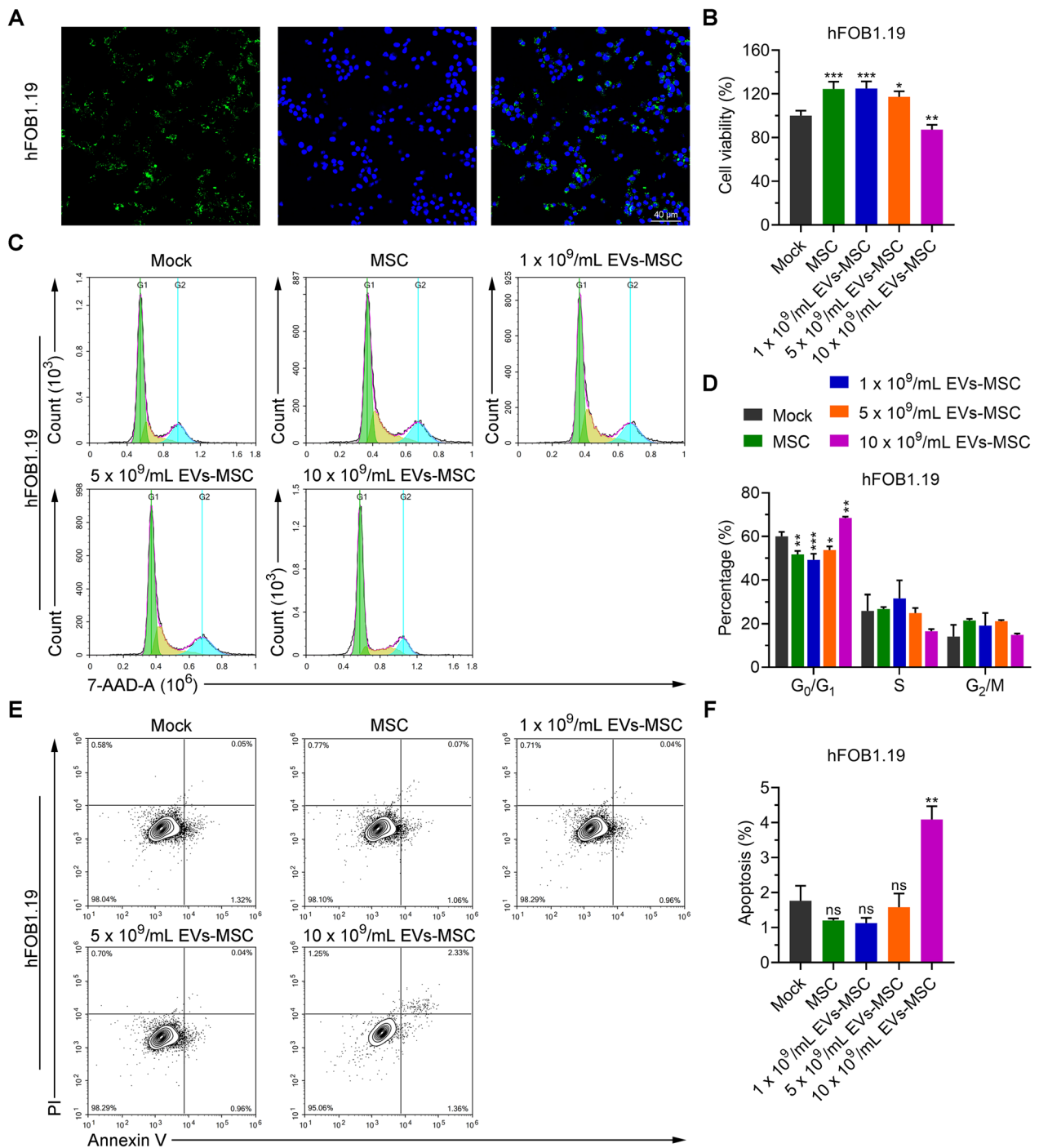


Fig. 2 A high concentration of hucMSC-exosomes inhibited the proliferation of osteoblasts. **A** Exosomes derived from hucMSCs were labeled with CFSE and the immunofluorescence of hFOB1.19 cells treated with the exosomes is shown. **B** Viability of hFOB1.19 cells cultured with MSCs and different concentrations of hucMSC-exosomes (EVs-MSC) as determined by MTT assay. **C, D** Cell cycle analysis of hFOB1.19 cells treated with hucMSCs or different concentrations of hucMSC-exosomes. **E, F** Cell apoptosis as analyzed by FITC-Annexin V kit and flow cytometry

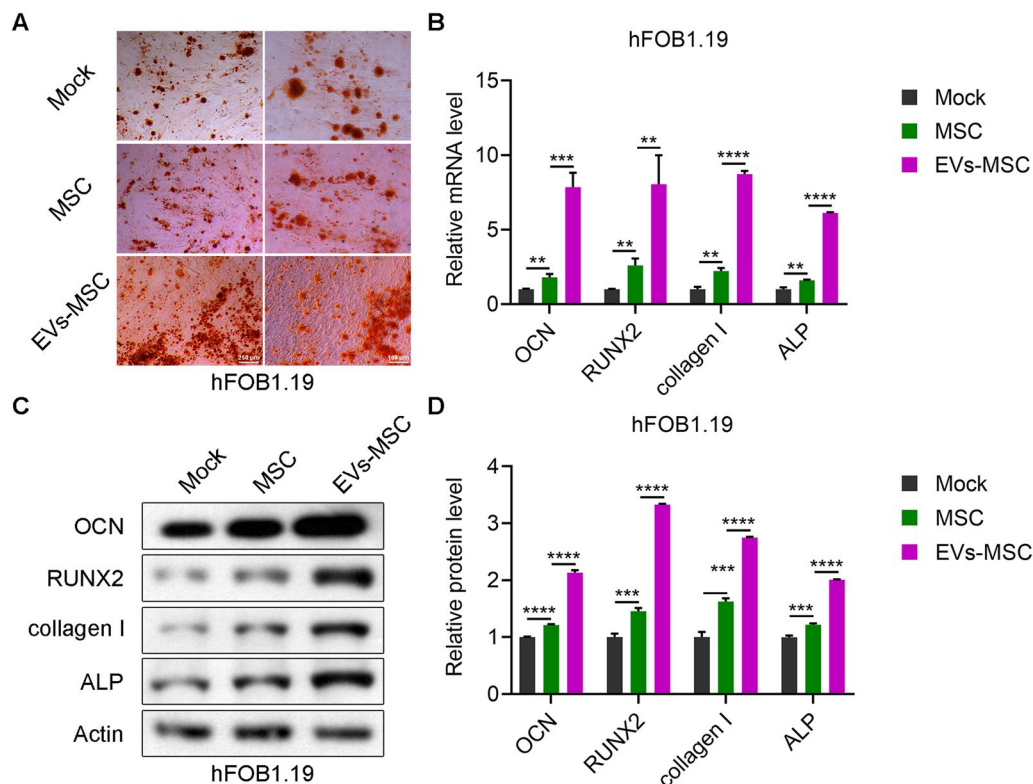


Fig. 3 hucMSCs and hucMSC-exosomes promote osteoblast differentiation. **A** Alizarin red staining of hFOB1.19 cells treated with hucMSCs and hucMSC-exosomes. **B** The mRNA expression levels of OCN, RUNX2, Collagen I, and ALP in hFOB1.19 cells treated with hucMSCs (MSC) or hucMSC-exosomes (EVs-MSC) as detected by RT-PCR. **C, D** Immunoblotting of OCN, RUNX2, collagen I, and ALP protein levels in hFOB1.19 cells treated with hucMSCs (MSC) or hucMSC-exosomes (EVs-MSC)

PRR34-AS1 in hFOB1.19 cells (Fig. 4D). Figure 4D illustrates that the relative expression level of LINC00520 in hFOB1.19 cells co-cultured with EVs-MSC was approximately 4-fold higher than that in hFOB1.19 cells without co-culture (Mock group), while the relative expression level of PRR34-AS1 in hFOB1.19 cells co-cultured with EVs-MSC was nearly 3-fold higher than that in hFOB1.19 cells without co-culture. Therefore, subsequent experiments were focused on the function of LINC00520 in hFOB1.19 cells.

LINC00520 in hucMSC-exosomes enhances osteoblast proliferation

We next determined whether exosomes from hucMSCs transfected with shLINC00520 or LINC00520 OE regulate osteoblast proliferation. Co-culturing hFOB1.19 cells with hucMSCs transfected with shLINC00520 resulted in the inhibition of LINC00520 expression in hFOB1.19 cells (Fig. 5A). Similarly, after hFOB1.19 cells were treated with exosomes which were obtained from

hucMSCs transfected with shLINC00520, the level of LINC00520 in hFOB1.19 cells was inhibited (Fig. 5A). Conversely, co-culturing hFOB1.19 cells with hucMSCs transfected with LINC00520 OE led to increased LINC00520 expression in hFOB1.19 cells (Fig. 5B). After hFOB1.19 cells were treated with exosomes which were obtained from hucMSCs transfected with LINC00520 OE, the level of LINC00520 in hFOB1.19 cells was increased (Fig. 5B). After hFOB1.19 cells were treated with exosomes from hucMSCs transfected with shLINC00520, the viability of hFOB1.19 cells was inhibited (Fig. 5C), and the cell cycle process of hFOB1.19 cells was arrested in the G_0/G_1 phase (Fig. 5D, E). When hFOB1.19 cells were treated with exosomes from hucMSCs transfected with LINC00520 OE, the viability of hFOB1.19 cells was promoted (Fig. 5C), and proportion of cells in the G_0/G_1 phase was decreased, indicating that cell cycle was accelerated (Fig. 5D, E). Compared with exosomes from hucMSCs transfected with shNC, exosomes from hucMSCs transfected with

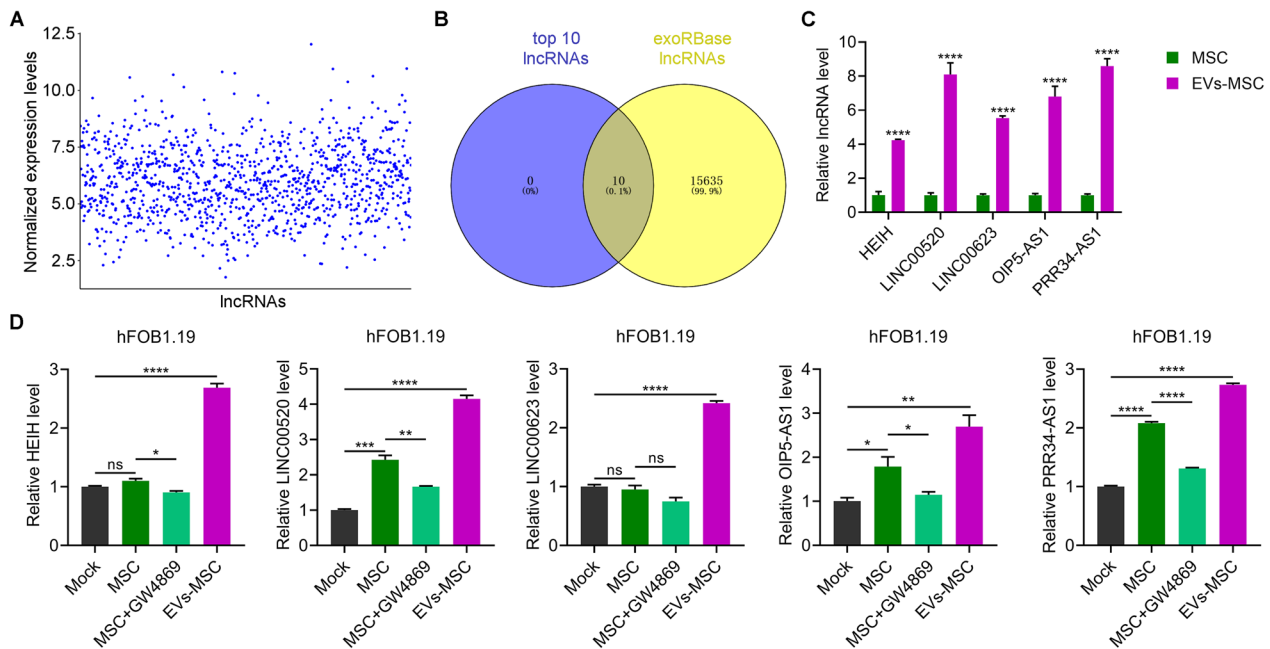


Fig. 4 Validation of the differentially expressed lncRNAs in hucMSC-exosomes. **A** Normalized lncRNA expression levels determined using bioinformatic methods. **B** Venn diagram of the top 10 expressed lncRNAs in hucMSCs (MSC) and the lncRNAs in the exoRBase database. **C** Relative expression of the lncRNAs HEIH, LINC00520, LINC00623, OIP5-AS1, and PRR34-AS1 in hucMSCs (MSC) or hucMSC-exosomes (EVs-MSC) as measured using RT-PCR. **D** Expression of HEIH, LINC00520, LINC00623, OIP5-AS1, and PRR34-AS1 in hFOB1.19 cells treated with MSC, MSC + GW4869 and EVs-MSC

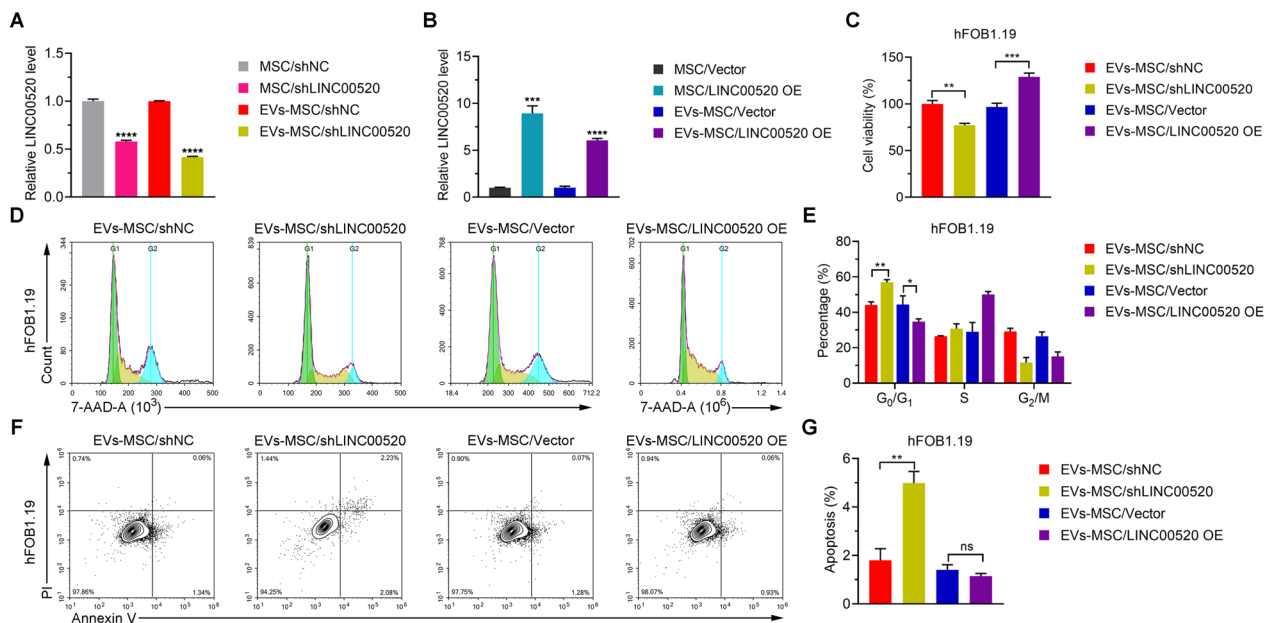


Fig. 5 LINC00520 in hucMSC-exosomes regulates the proliferation of osteoblasts. **A** Relative LINC00520 expression levels in hFOB1.19 cells exposed to hucMSCs transfected with a LINC00520 knockdown plasmid (MSC/shLINC00520) or the derived hucMSC-exosomes (EVs-MSC/shLINC00520) for 48 h. **B** Relative LINC00520 levels in hFOB1.19 cells exposed to hucMSCs transfected with a LINC00210 overexpression plasmid (MSC/LINC00520 OE) and the derived hucMSC-exosomes (EVs-MSC/LINC00520 OE) for 48 h. **C** Viability of hFOB1.19 cells treated with exosomes derived from hucMSCs transfected with a LINC00520 knockdown or LINC00520 overexpression plasmid. **D, E** Cell cycle analysis of hFOB1.19 cells treated with derived exosomes from hucMSCs transfected with a LINC00520 knockdown or LINC00520-overexpression plasmid. **F, G** Apoptosis of hFOB1.19 cells treated with derived exosomes from hucMSCs transfected with a LINC00520 knockdown or LINC00520-overexpression plasmid was analyzed using a FITC-Annexin V kit and flow cytometry

shLINC00520 promoted apoptosis of hFOB1.19 cells. However, there was no significant difference in the effect of exosomes from hucMSCs transfected with Vector and hucMSCs transfected with LINC00520 OE on the apoptosis of hFOB1.19 cells (Fig. 5F, G). Overall, these results suggest that manipulating LINC00520 expression in hucMSCs and subsequent treatment with their exosomes can influence the viability, cell cycle progression, and apoptosis of hFOB1.19 cells, highlighting the potential role of LINC00520 in osteoblast proliferation and function.

LINC00520 in hucMSC-exosomes promotes the formation of calcified nodules in hFOB1.19 cells

The above results show that LINC00520 has significant effects on osteoblast proliferation. Next, to determine whether LINC00520 affects the ability of hFOB1.19 cells to form mineralized bone, we treated hFOB1.19 cells with exosomes from hucMSCs transfected with shLINC00520 or LINC00520 OE plasmid and stained hFOB1.19 cells with alizarin red. Compared with the control cells, hFOB1.19 cells exposed to exosomes from hucMSCs transfected with shLINC00520 had fewer

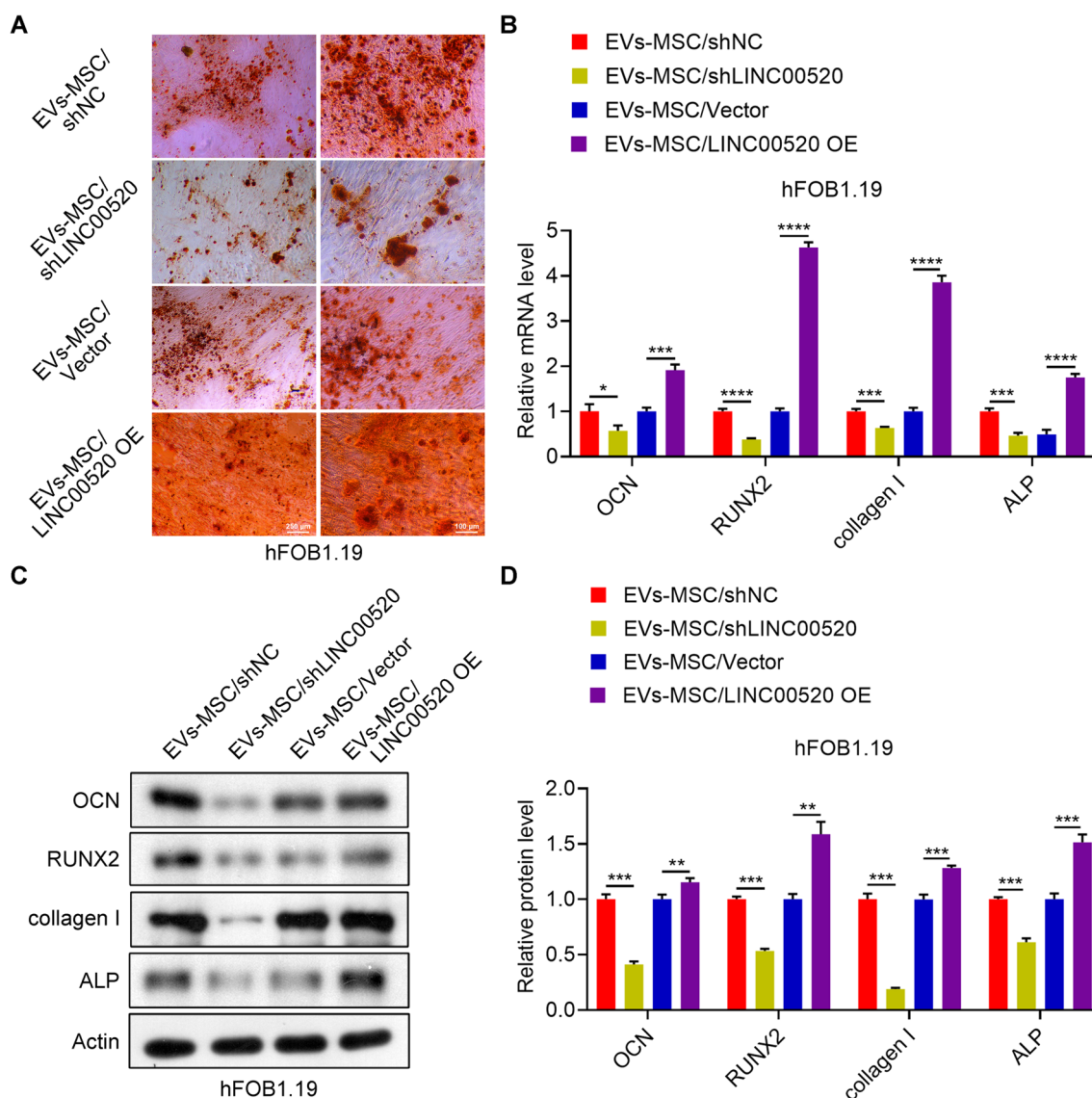


Fig. 6 LINC00520 in hucMSC-exosomes promotes osteoblast differentiation. **A** Alizarin red staining of hFOB1.19 cells treated with exosomes derived from hucMSCs transfected with a LINC00520 knockdown or overexpression plasmid. **B** Relative mRNA expression levels of OCN, RUNX2, collagen I, and ALP in hFOB1.19 cells cultured with exosomes derived from hucMSCs transfected with a LINC00520 knockdown or overexpression plasmid. **C, D** Relative protein levels of OCN, RUNX2, collagen I, and ALP in hFOB1.19 cells cultured exosomes derived from hucMSCs transfected with a LINC00520 knockdown or overexpression plasmid

calcified nodules, whereas more alizarin red staining was observed in hFOB1.19 cells exposed to exosomes from hucMSCs transfected with LINC00520 OE (Fig. 6A). The mRNA and protein expression levels of OCN, RUNX2, collagen I and ALP were significantly decreased in hFOB1.19 cells cultured with exosomes from hucMSCs transfected with shLINC00520 and were significantly increased in hFOB1.19 cells cultured with exosomes from hucMSCs transfected with LINC00520 OE (Fig. 6B, C, D).

Discussion

Slowing or stopping the progression of osteoporosis remains a significant clinical challenge. Understanding the molecular mechanisms underlying osteoporosis is crucial for identifying new therapeutic candidates. Since exosomes have been shown to be involved in various pathological processes [29, 30], the possible role of exosomes in osteoporosis has drawn extensive attention in recent years. Many studies have shown that co-culture with hucMSC-exosomes can alleviate osteoporosis [12, 31, 32], and exosomes derived from MSCs efficiently induced bone regeneration [33–35]. These findings suggest the potential application of exosomes for osteoporosis treatment. However, a study has shown that exosomes aggravate osteoporosis [36]. Thus, the effects of exosomes on osteoporosis remain controversial. Here, we successfully isolated hucMSC-exosomes and found that low concentration of hucMSC-exosomes promoted hFOB1.19 cell proliferation while high concentration of exosomes inhibited hFOB1.19 cell proliferation. These results expand our understanding of the effects of hucMSC-exosomes in osteoporosis.

LINC00520, located on chromosome 14, is overexpressed in breast cancer, nasopharyngeal carcinoma and laryngeal squamous cell carcinoma and promotes the development of these cancers [37]. Studies have also shown that LINC00520 inhibit the growth and metastasis of cutaneous squamous cell carcinoma [38]. Our study was the first to link LINC00520 with osteoblast proliferation and differentiation and found that LINC00520 promotes the proliferation and differentiation of hFOB1.19 cells. In addition, knockdown of LINC00520 induced G1 phase arrest, which may be due to its participation in the PI3k/AKT pathway [38]. Similarly, exosomes from hucMSCs with LINC00520 knockdown cause cell cycle arrest in hFOB1.19 cells in G1 phase.

In recent years, many studies have shown that LINC00520 is involved in the development and progression of disease by targeting multiple miRNAs, such as miR-4516, miR-1252-5p and miR-577 [39–41]. LINC00520 upregulates SOX5, FOXR2, or EIF5A2 through its interaction with miR-4516, miR-1252-5p, or miR-125b-5p, respectively [37, 39,

40]. This regulatory mechanism promotes cell proliferation and invasion in human hepatocellular carcinoma, accelerates the progression of lung adenocarcinoma, and enhances the proliferation and metastasis of malignant melanoma. Furthermore, LINC00520 increases the expression of POSTN, CCNE2, or HSP27 by targeting miR-577, thereby accelerating the progression of breast cancer, non-small cell lung cancer, or colorectal cancer [41–43]. In addition, LINC00520 promotes the development of acute kidney injury by targeting miR-27b-3p and regulating OSMR expression through the PI3K/AKT signaling pathway [44]. In this study, we found that exosomes from hucMSCs overexpressing LINC00520 promoted hFOB1.19 cell survival and the ability to form mineralized bone. Whether LINC00520 regulates mineralized bone-related genes in osteoblasts by targeting miRNAs remains to be further investigated.

This study has several limitations. First, because of the complexity of the exosome secretion and transmission mechanisms, further studies are necessary to confirm their function. Second, we only used hFOB1.19 cells to explore the effect of hucMSC-exosomes on osteoblast proliferation and osteogenic capacity, and an animal model was needed to further verify our findings [45].

Conclusions

In summary, hucMSC-exosomes regulate the proliferation and differentiation of osteoblasts via LINC00520. In hFOB1.19 cells, exosomes from hucMSCs down-regulated LINC00520 decreased cell viability and ability to form mineralized bone, blocked cell cycles, and increased apoptosis. Exosomes from hucMSCs overexpressing LINC00520 enhanced cell viability and the cell's ability to form mineralized bone and accelerated the cell cycle. These findings suggest that exosomes from hucMSCs overexpressing LINC00520 may be a novel therapeutic approach for osteoporosis.

Supplementary Information

The online version contains supplementary material available at <https://doi.org/10.1186/s13018-023-04021-y>.

Additional file 1: The original images of all immunoblotting in the study.

Acknowledgements

Not applicable.

Author contributions

JW and PT conceived and designed research; JW, LZ, HL, JZ, and PT performed the research; JW, LZ, HL, and JZ analyzed the data; JW wrote the paper; PT edited the manuscript. All authors approved final version of manuscript.

Funding

The study was supported by the Natural Science Foundation of Fujian (Grant Number: 2023J011836).

Data availability

LncRNA data from multiple myeloma-derived MSC was obtained from the gene expression omnibus (GSE118985, <https://www.ncbi.nlm.nih.gov/geo/query/acc.cgi?acc=GSE118985>). lncRNAs from exosome exoRBase (<http://www.exorbase.org/>) was used to predict lncRNAs regulating osteoblast differentiation in exosomes. Other datasets used or analyzed during this study are available from the corresponding author on reasonable request.

Declarations**Ethics approval and consent to participate**

Not applicable.

Consent for publication

Not applicable.

Competing interests

No competing interests were involved in this study.

Received: 13 January 2023 Accepted: 15 July 2023

Published online: 29 July 2023

References

- Rachner TD, Khosla S, Hofbauer LC. Osteoporosis: now and the future. *Lancet*. 2011;377(9773):1276–87.
- Golub EE. Biomineralization and matrix vesicles in biology and pathology. *Semin Immunopathol*. 2011;33(5):409–17.
- Keller S, Sanderson MP, Stoock A, Altevogt P. Exosomes: from biogenesis and secretion to biological function. *Immunol Lett*. 2006;107(2):102–8.
- Taylor DD, Gerceel-Taylor C. MicroRNA signatures of tumor-derived exosomes as diagnostic biomarkers of ovarian cancer. *Gynecol Oncol*. 2008;110(1):13–21.
- Al-Nedawi K, Meehan B, Micallef J, Lhotak V, May L, Guha A, et al. Intercellular transfer of the oncogenic receptor EGFRvIII by microvesicles derived from tumour cells. *Nat Cell Biol*. 2008;10(5):619–24.
- Luketic L, Delanghe J, Sobol PT, Yang P, Frotten E, Mossman KL, et al. Antigen presentation by exosomes released from peptide-pulsed dendritic cells is not suppressed by the presence of active CTL. *J Immunol* (Baltimore, Md: 1950). 2007;179(8):5024–32.
- Balaj L, Lessard R, Dai L, Cho Y-J, Pomeroy SL, Breakefield XO, et al. Tumour microvesicles contain retrotransposon elements and amplified oncogene sequences. *Nat Commun*. 2011;2:180.
- Narayanan R, Huang C-C, Ravindran S. Hijacking the cellular mail: exosome mediated differentiation of mesenchymal stem cells. *Stem Cells Int*. 2016;2016:3808674.
- Inder KL, Ruelcke JE, Petelin L, Moon H, Choi E, Rae J, et al. Cavin-1/PTRF alters prostate cancer cell-derived extracellular vesicle content and internalization to attenuate extracellular vesicle-mediated osteoclastogenesis and osteoblast proliferation. *J Extracell Vesicles*. 2014;3:23784.
- Kawakubo A, Matsunaga T, Ishizaki H, Yamada S, Hayashi Y. Zinc as an essential trace element in the acceleration of matrix vesicles-mediated mineral deposition. *Microsc Res Tech*. 2011;74(12):1161–5.
- Ding D-C, Chang Y-H, Shyu W-C, Lin S-Z. Human umbilical cord mesenchymal stem cells: a new era for stem cell therapy. *Cell Transplant*. 2015;24(3):339–47.
- Hu Y, Zhang Y, Ni C-Y, Chen C-Y, Rao S-S, Yin H, et al. Human umbilical cord mesenchymal stromal cells-derived extracellular vesicles exert potent bone protective effects by CLEC11A-mediated regulation of bone metabolism. *Theranostics*. 2020;10(5):2293–308.
- Huang J, U KP, Yang F, Ji Z, Lin J, Weng Z, et al. Human pluripotent stem cell-derived ectomesenchymal stromal cells promote more robust functional recovery than umbilical cord-derived mesenchymal stromal cells after hypoxic-ischaemic brain damage. *Theranostics*. 2022;12(1):143–66.
- Xie Q, Liu R, Jiang J, Peng J, Yang C, Zhang W, et al. What is the impact of human umbilical cord mesenchymal stem cell transplantation on clinical treatment? *Stem Cell Res Ther*. 2020;11(1):519.
- Ko N-Y, Chen L-R, Chen K-H. The role of micro RNA and long-non-coding RNA in osteoporosis. *Int J Mol Sci*. 2020;21(14):4886.
- Tye CE, Boyd JR, Page NA, Falcone MM, Stein JL, Stein GS, et al. Regulation of osteogenesis by long noncoding RNAs: an epigenetic mechanism contributing to bone formation. *Connect Tissue Res*. 2018;59(sup1):35–41.
- Gu X, Li M, Jin Y, Liu D, Wei F. Identification and integrated analysis of differentially expressed lncRNAs and circRNAs reveal the potential ceRNA networks during PDLSC osteogenic differentiation. *BMC Genet*. 2017;18(1):100.
- Yang X, Yang J, Lei P, Wen T. LncRNA MALAT1 shuttled by bone marrow-derived mesenchymal stem cells-secreted exosomes alleviates osteoporosis through mediating microRNA-34c/SATB2 axis. *Aging (Albany NY)*. 2019;11(20):8777–91.
- Li DJ, Liu GQ, Xu XJ. Silence of lncRNA BCAR4 alleviates the deterioration of osteoporosis. *Eur Rev Med Pharmacol Sci*. 2020;24(11):5905–13.
- Yu X, Rong P-Z, Song M-S, Shi Z-W, Feng G, Chen X-J, et al. lncRNA SNHG1 induced by SP1 regulates bone remodeling and angiogenesis via sponging miR-181c-5p and modulating SFRP1/Wnt signaling pathway. *Mol Med*. 2021;27(1):141.
- Ren L, Guo L, Kou N, Lv J, Wang Z, Yang K. LncRNA LINC00963 promotes osteogenic differentiation of hBMSCs and alleviates osteoporosis progression by targeting miRNA-760/ETS1 axis. *Autoimmunity*. 2021;54(6):313–25.
- Ren Y, Zhang K, Wang J, Meng X, Du X, Shi Z, et al. HOTAIRM1 promotes osteogenic differentiation and alleviates osteoclast differentiation by inactivating the NF- κ B pathway. *Acta Biochim Biophys Sin (Shanghai)*. 2021;53(2):201–11.
- Zhang Q, Shen J, Wu Y, Ruan W, Zhu F, Duan S. LINC00520: a potential diagnostic and prognostic biomarker in cancer. *Front Immunol*. 2022;13:845418.
- Luberto C, Hassler DF, Signorelli P, Okamoto Y, Sawai H, Boros E, et al. Inhibition of tumor necrosis factor-induced cell death in MCF7 by a novel inhibitor of neutral sphingomyelinase. *J Biol Chem*. 2002;277(43):41128–39.
- Chen L, Brigstock DR. Integrins and heparan sulfate proteoglycans on hepatic stellate cells (HSC) are novel receptors for HSC-derived exosomes. *FEBS Lett*. 2016;590(23):4263–74.
- Fyfe I. Exosomes can spread toxic AD pathology. *Nat Rev Neurol*. 2018;14(8):451.
- Schinke C, Qu P, Mehdi SJ, Hoering A, Epstein J, Johnson SK, et al. The pattern of mesenchymal stem cell expression is an independent marker of outcome in multiple myeloma. *Clin Cancer Res*. 2018;24(12):2913–9.
- Lallemand T, Rouahi M, Swiader A, Grazide M-H, Geoffre N, Alayrac P, et al. nSMase2 (type 2-neutral sphingomyelinase) deficiency or inhibition by GW4869 reduces inflammation and atherosclerosis in ApoE^{-/-} mice. *Arterioscler Thromb Vasc Biol*. 2018;38(7):1479–92.
- Kalluri R, LeBleu VS. The biology function and biomedical applications of exosomes. *Science*. 2020;367(6478):eaau6977.
- Zhang L, Yu D. Exosomes in cancer development, metastasis, and immunity. *Biochim Biophys Acta Rev Cancer*. 2019;1871(2):455–68.
- Yahao G, Xinjia W. The role and mechanism of exosomes from umbilical cord mesenchymal stem cells in inducing osteogenesis and preventing osteoporosis. *Cell Transplant*. 2021;30:9636897211057464.
- Liang M, Liu W, Peng Z, Lv S, Guan Y, An G, et al. The therapeutic effect of secretome from human umbilical cord-derived mesenchymal stem cells in age-related osteoporosis. *Artif Cells Nanomed Biotechnol*. 2019;47(1):1357–66.
- Chen S, Tang Y, Liu Y, Zhang P, Lv L, Zhang X, et al. Exosomes derived from miR-375-overexpressing human adipose mesenchymal stem cells promote bone regeneration. *Cell Prolif*. 2019;52(5):e12669.
- Furuta T, Miyaki S, Ishitobi H, Ogura T, Kato Y, Kamei N, et al. Mesenchymal stem cell-derived exosomes promote fracture healing in a mouse model. *Stem Cells Transl Med*. 2016;5(12):1620–30.
- Guo S-C, Tao S-C, Yin W-J, Qi X, Sheng J-G, Zhang C-Q. Exosomes from human synovial-derived mesenchymal stem cells prevent glucocorticoid-induced osteonecrosis of the femoral head in the rat. *Int J Biol Sci*. 2016;12(10):1262–72.
- Yu L, Hu M, Cui X, Bao D, Luo Z, Li D, et al. M1 macrophage-derived exosomes aggravate bone loss in postmenopausal osteoporosis via a microRNA-98/DUSP1/JNK axis. *Cell Biol Int*. 2021;45(12):2452–63.

37. Luan W, Ding Y, Yuan H, Ma S, Ruan H, Wang J, et al. Long non-coding RNA LINC00520 promotes the proliferation and metastasis of malignant melanoma by inducing the miR-125b-5p/EIF5A2 axis. *J Exp Clin Cancer Res CR*. 2020;39(1):96.
38. Mei X-L, Zhong S. Long noncoding RNA LINC00520 prevents the progression of cutaneous squamous cell carcinoma through the inactivation of the PI3K/Akt signaling pathway by downregulating EGFR. *Chin Med J (Engl)*. 2019;132(4):454–65.
39. Li Q, Wang W, Yang T, Li D, Huang Y, Bai G, et al. LINC00520 up-regulates SOX5 to promote cell proliferation and invasion by miR-4516 in human hepatocellular carcinoma. *Biol Chem*. 2022;403(7):665–78.
40. Chen X, Chen H, Liu M, Xiong J, Song Z. Long noncoding RNA LINC00520 accelerates lung adenocarcinoma progression via miR-1252-5p/FOXR2 pathway. *Hum Cell*. 2021;34(2):478–90.
41. Guo Y, Feng L. N6-methyladenosine-mediated upregulation of LINC00520 accelerates breast cancer progression via regulating miR-577/POSTN axis and downstream ILK/AKT/mTOR signaling pathway. *Arch Biochem Biophys*. 2022;729:109381.
42. Wang JF, Xi ZN, Su HJ, Bao Z, Qiao YH. SP1-induced overexpression of LINC00520 facilitates non-small cell lung cancer progression through miR-577/CCNE2 pathway and predicts poor prognosis. *Hum Cell*. 2021;34(3):952–64.
43. Jin XH, Hong YG, Li P, Hao LQ, Chen M. Long noncoding RNA LINC00520 accelerates the progression of colorectal cancer by serving as a competing endogenous RNA of microRNA-577 to increase HSP27 expression. *Hum Cell*. 2020;33(3):683–94.
44. Tian X, Ji Y, Liang Y, Zhang J, Guan L, Wang C. LINC00520 targeting miR-27b-3p regulates OSMR expression level to promote acute kidney injury development through the PI3K/AKT signaling pathway. *J Cell Physiol*. 2019;234(8):14221–33.
45. Komori T. Animal models for osteoporosis. *Eur J Pharmacol*. 2015;759:287–94.

Publisher's Note

Springer Nature remains neutral with regard to jurisdictional claims in published maps and institutional affiliations.

Ready to submit your research? Choose BMC and benefit from:

- fast, convenient online submission
- thorough peer review by experienced researchers in your field
- rapid publication on acceptance
- support for research data, including large and complex data types
- gold Open Access which fosters wider collaboration and increased citations
- maximum visibility for your research: over 100M website views per year

At BMC, research is always in progress.

Learn more biomedcentral.com/submissions

